Motion of an articulated straw along a vibrating rod

Hiroshi Takano[1]

[1] *Educational Studies on Natural Science and ICT, Joetsu University of Education*
1 Yamayashiki-cho, Joetsu, Niigata, 943-8512, Japan [*]

(Dated: Oct. 14, 2023)

Abstract— When an articulated drinking straw is slid over a rod vibrated by a motor, the straw moves up and down continuously. To clarify the mechanism for this motion, a straw was created that was narrower at the center than at the ends and the mechanism for the up-and-down motion as well as its reversal at the rod tip was examined. The angle ψ between the rod and the straw is constant because they are in contact at three points, i.e., at both ends and the center. Therefore, when the straw rotates around the rod, it will move unidirectionally according to the sign of ψ. This velocity is determined as a function of the straw half-length and the number of rotations of the nut to which the rod is attached. As the straw rises, the rod tip enters the straw, and the ascent stops when ψ reaches zero because the rate of ascent is proportional to ψ. The sign of ψ then reverses to start the downward motion, and the straw returns. When it reaches a reflector disk, the sign of ψ reverses again and the straw rises. Experiments were conducted to measure the velocities of three straws with different lengths, and the results showed that the theoretical velocities were greater than the experimental ones. The reason for this is assumed to be that although in theory the straw does not slip at the point of contact between its center and the rod, in reality it does slip. However, the theoretical and experimental velocities decreased in similar ways with increasing straw half-length, and the agreement between them was determined by the relative error. For half-lengths below 1.0 cm, the average agreement was approx. 80%, and for all lengths it was approx. 73%. The agreement would have been even better if it had not been for the effects of slippage between the straw and the rod, the presence of nodes and antinodes of the rod vibration, and deformation in the central portion of straw. Considering these effects, the experimental values support the validity of the mechanistic considerations of the straw motion and the theoretically determined velocity.

I. INTRODUCTION

The artist Keijiro Sato [1] created various moving works of art, one of which involved a vibrating rod passing through a Styrofoam ball, whereupon the ball mysteriously moves up and down. Sato's work entitled "Gifu Susuki Clump'99 (Susuki: Pampas Grass)" has 41 of these in a row [2]. Inspired by this, the present author made a vibrating rod and slid a Styrofoam ball over it to reproduce the up-and-down motion; see the corresponding online video [3]. However, although that attempt reproduced the effect, sometimes it worked and sometimes it did not. When the author was looking for something else that would work, he happened on a drinking straw on his desk and slid that over the rod, whereupon it surprisingly also moved slowly along the rod. This straw was a flexible straw with an articulated section as shown in Fig. 1; when a nonarticulated straw was used, no vertical motion occurred.

FIG. 1. Flexible straws that bend at the articulated section.

[*] Email: takano@juen.ac.jp

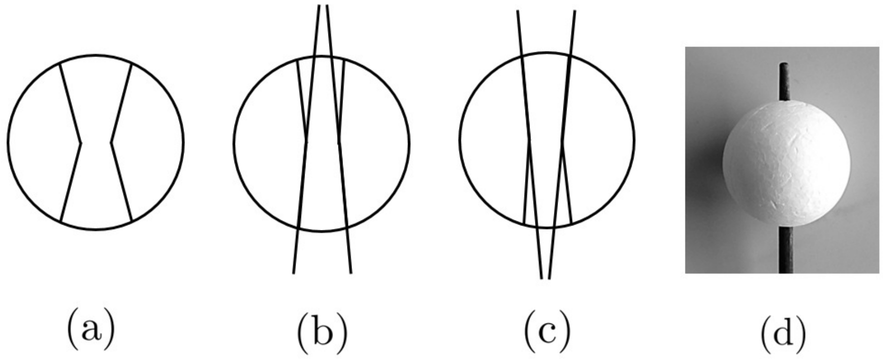

FIG. 2. (a) Schematic of internal structure of Styrofoam sphere. (b) Chopstick inserted from below. (c) Chopstick inserted from above. (d) Photograph of actual insertion of chopstick.

Because the articulated section seemed to be slightly narrower than the rest of the straw, the author speculated that this difference might be the cause of the vertical motion. This speculation was based on the author knowing that the hole in the Styrofoam sphere was not actually a simple cylinder. Its structure is shown schematically in Fig. 2(a), where the center is narrower than the ends and the hole is slightly conical. The author learned of this structure from museum staff when he visited the Museum of Fine Arts, Gifu for an exhibition of Sato's works in November 2016. Then, to reproduce the movement of the Styrofoam sphere, one with a 2-mm-diameter hole and a 2-mm-diameter rod were purchased. However, as the hole and rod had the same diameter, the hole in the Styrofoam ball had to be enlarged. Therefore, using a chopstick normally used for eating (the author is Japanese), the hole was enlarged by inserting the chopstick into each end, whereupon the vertical movement was reproduced. The hole that was produced was not made with the structure of Fig. 2(a) in mind, but because the chopstick was thinner at its tip, the ends of the hole through which the chopstick was inserted became wider than the center, as shown in Fig. 2(b) and (c). Then, the author noticed that the interior had the structure shown in Fig. 2(a) and realized again that this structure is important for the vertical motion.

To examine the motion of the straw, various ones were made with different distances from the articulated section to the end, and experiments showed that the shorter the distance, the faster the vertical motion. Straws were also created so that the ends had different diameters, and experiments showed that the resulting motion was only ever in the direction from the wider opening to the narrower one. Furthermore, it was confirmed that a similar motion occurred when a paper cup with its bottom removed was passed over a rod that was then rotated by hand. These observations raise the following two questions: why does using a straw with an articulated section result in vertical motion, and why does using a straw with different widths result in unidirectional motion? The purpose of this paper is to answer the first question, with the second question discussed in another paper [4].

Herein, Section II shows the demonstration setup and describes the motions of straws whose articulated section is of differing length, straws with a narrower center, and straws whose ends have different widths. Section III examines the mechanism for the up-and-down motion of a straw with a narrower center and its reversal upon reaching the end of the rod, and the velocity of motion is determined theoretically. In Section IV, experimentally measured velocities are compared with the theoretical values. Finally, the paper concludes with Section V.

II. DEMONSTRATION OF STRAW MOTION

A. Demonstration Setup

As shown in Fig. 3(a), a nut was attached to the shaft of a motor (Mabuchi motor RE-260RA). As seen in Fig. 3(b), the inner diameter of the nut was 6 mm, its outside was hexagonal with a side length of 10 mm. The center B of the nut and the axis A of the motor were offset by approx. 1.5 mm. As shown in Fig. 4(a), the rod was attached to the side of the motor with double-sided tape, and then more tape was applied to hold the rod in place as shown in Fig. 4(b).

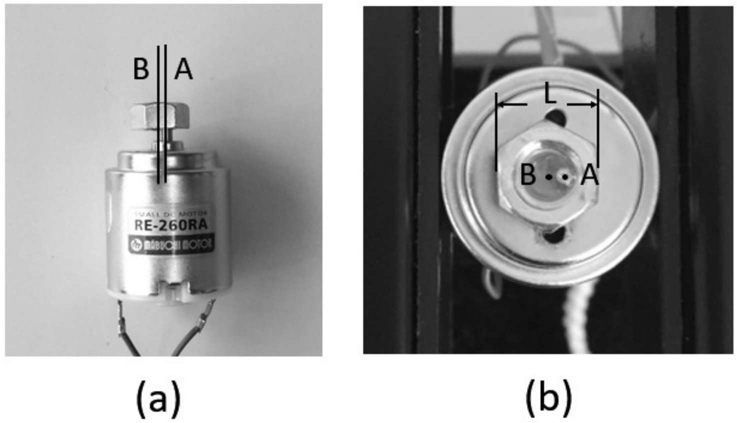

FIG. 3. (a) Side view of motor: line A is the center line of the motor shaft, line B is the center line of the nut, and as can be seen, there is a slight offset between the two. (b) Top view: point A is the center of the motor shaft, and point B is the center of the nut. L is 10 mm

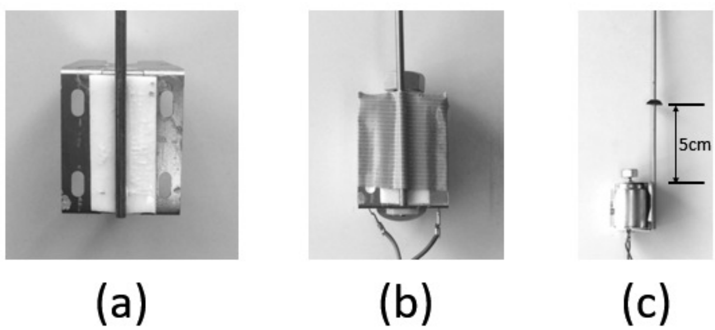

FIG. 4. (a) Double-sided tape used to attached rod to side of motor. (b) Rod held in place with more tape. (c) Reflective disk made of paper is attached to rod 5 cm from top of motor.

Because the center of the nut and the motor's axis of rotation were slightly offset from each other, when the nut rotated, the motor and hence the attached rod moved orbitally. This orbital motion then caused the straw to rotate about its own axis, resulting in the observed motion along the rod. As shown in Fig. 4(c), a paper disk was attached to the rod at 5 cm from the top of the motor to prevent the straw from descending beyond that point. The rod was 2-mm thick and made of brass, and it extended to 22 cm from the top of the motor.

As shown in Fig. 5(a), the motor was wrapped in a cushioning material made of polyurethane; this was wound to a diameter of approx. 6 cm [Fig. 5(b)] and then clamped in a stand [Fig. 5(c)]. Wrapping the motor in this cushioning material allowed the rod to move orbitally in accordance with the orbital motion of the nut. As shown in Fig. 5(c), the motor was connected to a power supply that applied voltage to the motor controllably in the range of 1.5-3 V.

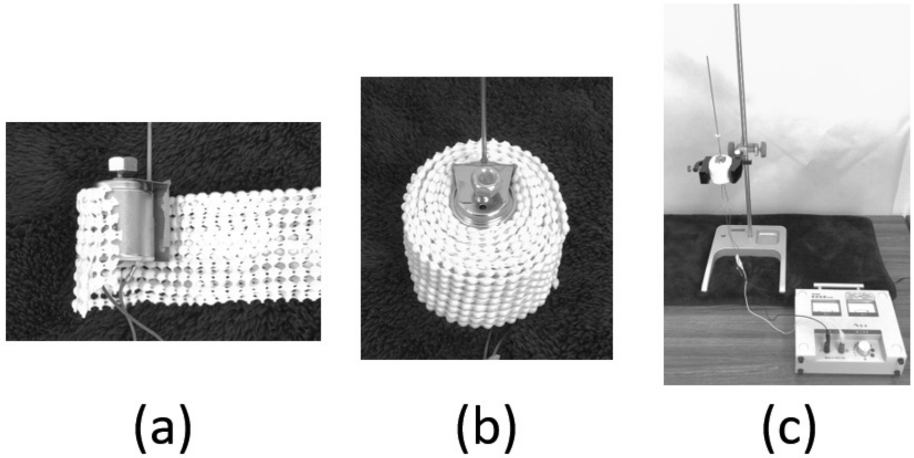

FIG. 5. (a) Motor being wrapped in polyurethane cushioning material to (b) a diameter of approx. 6 cm. (c) Motor connected to power supply.

B. Various Straw Motions

The first straw used in the demonstration had an inner diameter of 6 mm and was cut to the chosen length with the articulated section in the center, as shown in Fig. 6(a). The total length of the straw was 44 mm, and the length of the articulated section was 8 mm. The straw was slid over the rod, then the motor was activated with an applied voltage of approx. 2.5 V. The straw rose initially to the top of the rod and then descended; when it touched the reflector disk near the bottom of the rod, it reversed its direction of motion and rose again. This motion repeated and is shown in Fig. 7 as frames from a corresponding online video [5]. Other online videos show that this motion also occurred when the rod was horizontal [6] or upside down [7], and the reversal of motion at the rod tip is astonishing.

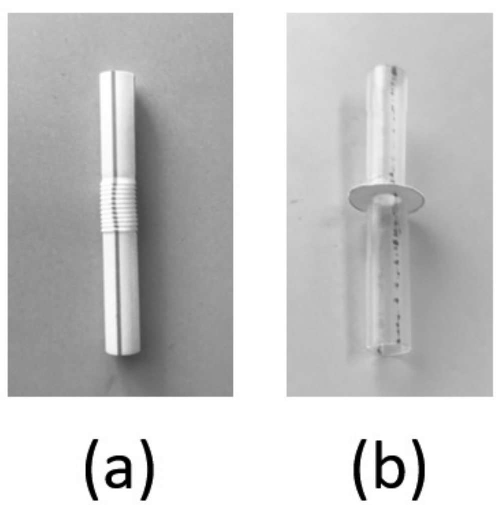

FIG. 6. (a) Straw with a total length of 44 mm and an 8-mm-long articulated section in its center. (b) Straw made from two short sections connected by a piece of paper containing a circular hole narrower than the connected straw sections.

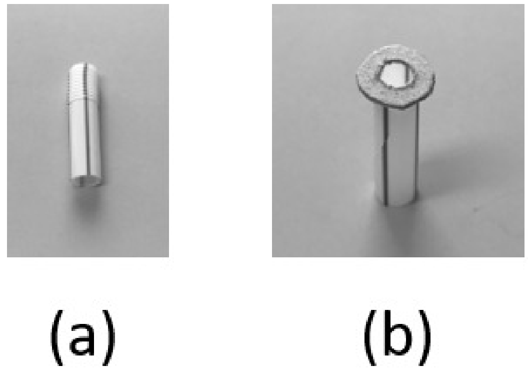

FIG. 8. (a) Short straw cut just above articulated section. (b) Second short straw with no articulated section but with a piece of paper at one end containing a narrower circular hole.

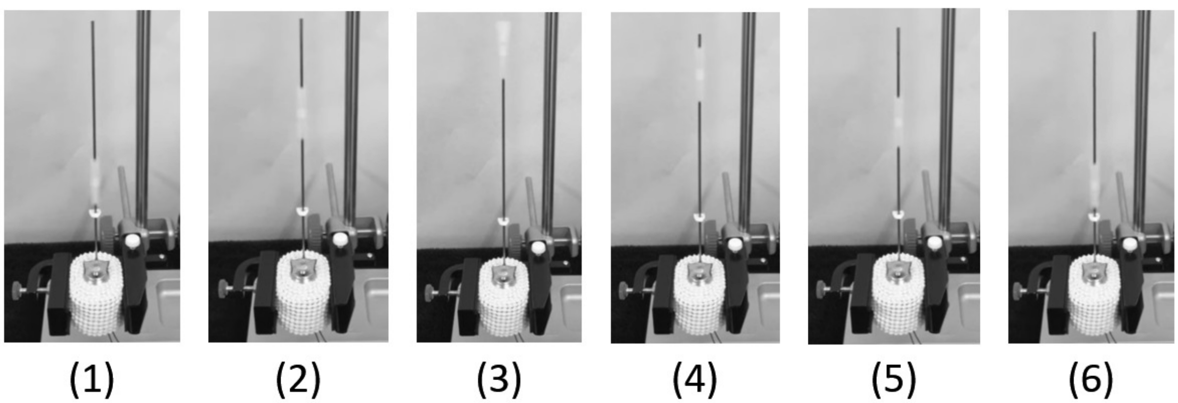

FIG. 7. Vertical motion of straw with articulated section in its center.

A possible reason why the straw with the articulated section moved up and down on the rod is that it was slightly narrower at the articulated section. Therefore, a second straw was prepared as shown in Fig. 6(b), made from two short sections connected by a piece of paper containing a circular hole narrower than the connected straw sections. As shown in the corresponding online video, this straw exhibited similar motion [8].

This raised the question of what would happen with a straw whose ends had different radii. Therefore, a straw cut just above the articulated section was prepared and tested, and it moved only in the direction from the wider end to the narrower end; see the corresponding online video [9]. As can be seen in the video, the straw stopped rising at a node of vibration along the rod (as discussed in Section IV); if poked by hand, it continued to rise and then flew off when it reached the rod tip. In addition, as shown in Fig. 8(b), a second short straw was prepared with no articulated section but with a piece of paper at one end containing a narrower circular hole. As can be seen in the corresponding online video [10], the same motion was observed for this straw; however, it could pass through the node, or it could stop at the tip and not fly off.

The straws moved too quickly to be observed in detail with the commercial camera that was available. Therefore, a search was made for something that could reproduce the motion but slower, and it was decided to use a paper cup. When the bottom of a paper cup is removed, it becomes a cylinder with differing radius. Such a cup was passed over a wooden rod (12 mm in diameter) that was then turned by hand. When the rod was vertical, the paper cup slid and did not rise, but when the rod was horizontal, the cup moved along it. Therefore, a strip of rubber (cut from that used on table-tennis equipment) was attached around the smaller inner circumference to create greater friction with the rod. With this cup, it was confirmed that whether the rod was horizontal or vertical when turned, the cup moved in the direction from wider to narrower; see the corresponding online video [11]. However, although the motions of various straws and cups have been presented, as noted in Section I only the motions of straws with a narrower center are discussed herein.

III. MOTIONS OF STRAWS WITH A NARROWER CENTER

A. Analysis of Vertical Motion

Figure 9(a) shows the model straw considered herein, with center radius $\bar{l}_1$, end radius $\bar{l}_2$, and length $2\bar{l}_4$ on a rod of radius $\bar{l}_3$. As shown in Fig. 9(b), the bottom circumference of the straw is C_2, the center circumference is C_1, and the top circumference is C_3.

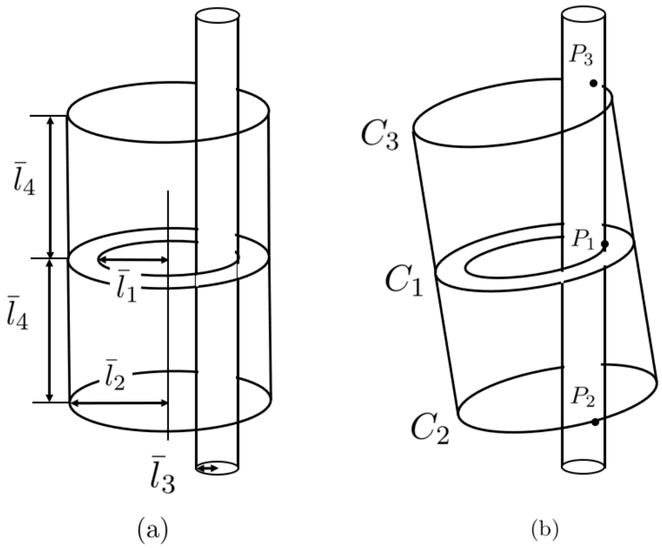

FIG. 9. (a) Dimensions of model straw and rod. (b) Straw makes contact with rod at points P_1, P_2, and P_3. The bottom circumference of the straw is C_2, the center circumference is C_1, and the top circumference is C_3.

When the axis of the motor rotates counterclockwise, so does the nut, and because the nut is off-center from the motor, the motor executes counterclockwise orbital motion. The rod attached to the motor rotated counterclockwise orbital motion, whereupon the straw rotates counterclockwise about its own axis. If the motor were to rotate clockwise, then so would be all the other motions. Hereinafter, counterclockwise motor rotation is considered without loss of generality because the direction of motor rotation is not an essential factor for vertical motion.

The first thing to consider is the contact between the rod and the straw. A stable way of making contact during rapid rotation is to have contact with the rod at three points on the respective straw circumferences C_1, C_2, and C_3 as shown in Fig. 9(b), with the contact points denoted as P_1, P_2, and P_3, respectively. Figure 10(a)–(c) show this situation from the directions parallel to the $\boldsymbol{e}_3, \boldsymbol{e}_1$, and $\boldsymbol{e}_2$ axes, respectively. If the principal axis of inertia of the straw is $\bar{\boldsymbol{e}}_{(i=1,2,3)}$, then $\boldsymbol{e}_{(i=1,2,3)}$ is that axis rotated about the $\bar{\boldsymbol{e}}_3$ axis so that $\boldsymbol{e}_1$ always points toward contact point P_1.

Figure 10(a) shows the rod and straw projected onto the plane containing circumference C_3. The cross section of the rod in the plane containing C_3 is an ellipse, which is D_3, and its midpoint is P_{D3}. In Fig 10(b), the angle between (i) the line passing through the origin of the $\boldsymbol{e}$ system and point P_{D3} (i.e., the center line of the rod) and (ii) the $\boldsymbol{e}_3$ axial direction is defined as ψ and is negative in this situation.

That the straw and rod are in contact at three points is supported by video evidence. The motion was captured at 1,000 fps with a digital camera (CASIO EX-ZR200), and in Fig. 11 shows frames from that video. In particular, frames 1, 5, 9, 12, and 15 show the straw at an angle to the rod, corresponding to Fig. 10(b).

The angle between the rod and the straw can be obtained approximately. In Fig. 10(a), the cross section of the rod is approximated as a circle of radius $\bar{l}_3$, which is shown in Fig. 12(a). There, the center of the section of the rod in contact at point P_1 is P_{D1}, the center of the straw is G, and the angle between lines GP_{D3} and GP_{D1} is $\alpha > 0$. By approximating the cross section as a circle, the length of GP_{D3} is $\bar{l}_2 - \bar{l}_3$ and the length of GP_{D1} is $\bar{l}_1 - \bar{l}_3$. Therefore, because

$$(\bar{l}_2 - \bar{l}_3)\cos\alpha = (\bar{l}_1 - \bar{l}_3), \tag{1}$$

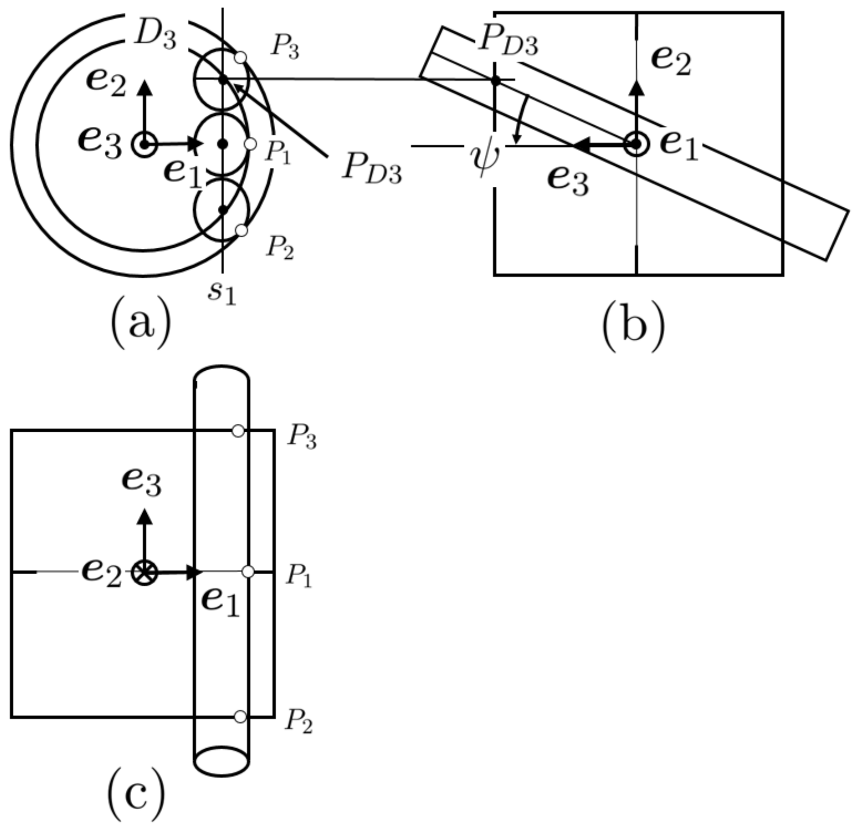

FIG. 10. (a) View parallel to $\boldsymbol{e}_3$ axis. The rod and straw are projected onto the plane containing circumference C_3. The cross section of the rod in the plane containing C_3 is an ellipse, which is D_3, and its midpoint is P_{D3}. (b) View parallel to $\boldsymbol{e}_1$ axis. The angle between the line passing through the origin of the $\boldsymbol{e}$ system and point P_{D3} (i.e., the center line of the rod) and the $\boldsymbol{e}_3$ axial direction is defined as ψ and is negative in this situation. (c) View parallel to $\boldsymbol{e}_2$ axis.

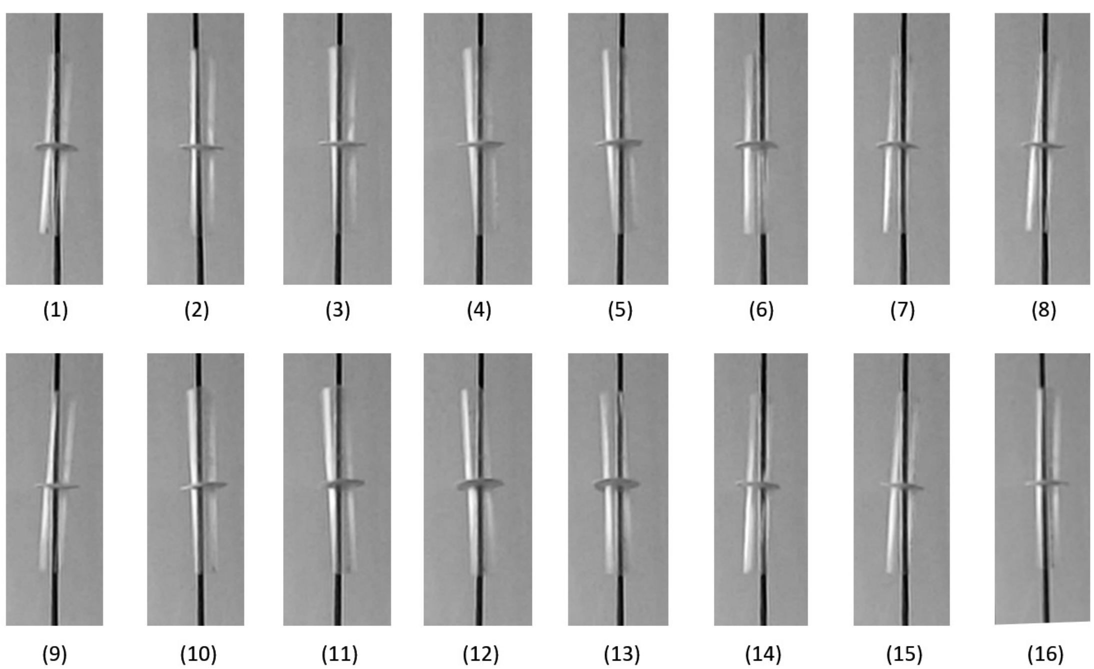

FIG. 11. Frames from video of motion captured at 1,000 fps with a digital camera (CASIO EX-ZR200).

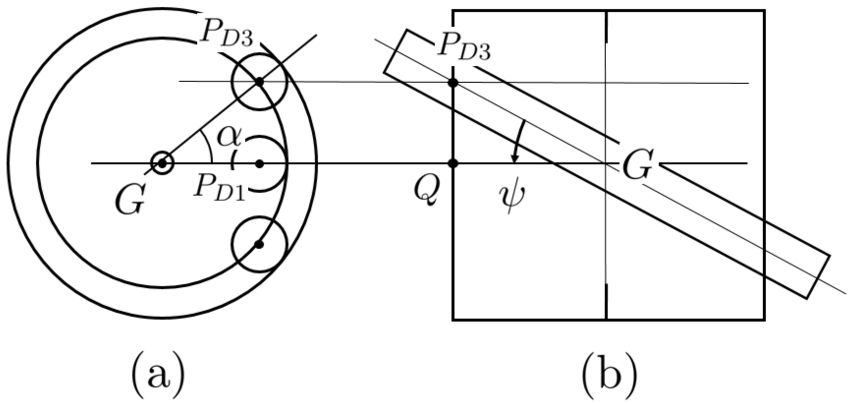

FIG. 12. (a) Center of section of rod in contact at point P_1 is P_{D1}, and center of straw is G. The angle between lines GP_{D3} and GP_{D1} is $\alpha > 0$. (b) View parallel to $\boldsymbol{e}_1$ axis.

we have

$$\sin\alpha = \sqrt{1 - \left(\frac{\bar{l}_1 - \bar{l}_3}{\bar{l}_2 - \bar{l}_3}\right)^2}. \tag{2}$$

In Fig. 12(b), the length of GQ is $\bar{l}_4$ and the length of QP_{D3} is $(\bar{l}_2 - \bar{l}_3)\sin\alpha > 0$, so substituting Eq. (2), we obtain $\tan\psi$ as

$$\begin{aligned}\tan\psi &= -\frac{|QP_{D3}|}{|GQ|}\\ &= -\frac{(\bar{l}_2 - \bar{l}_3)\sin\alpha}{\bar{l}_4}\\ &= -\frac{\sqrt{(\bar{l}_2 - \bar{l}_3)^2 - (\bar{l}_1 - \bar{l}_3)^2}}{\bar{l}_4},\end{aligned} \tag{3}$$

where here we have $\psi < 0$, so the right-hand side has a negative sign. Thus, as an approximation to ψ, we obtain

$$\psi = \arctan\left(-\frac{1}{\bar{l}_4}\sqrt{(\bar{l}_2 - \bar{l}_3)^2 - (\bar{l}_1 - \bar{l}_3)^2}\right). \tag{4}$$

Now, let us consider whether the straw is sliding against the rod at the contact point. It is difficult to imagine the motion of a straw rotating while in contact with a rod, so let us first consider the case where the straw and rod are parallel and in contact only at P_1. Then, let us see how P_1 moves and accordingly how $\bar{\boldsymbol{e}}_i$ (principal axes of inertia) and $\boldsymbol{e}_i$ rotate when the rod is fixed and the straw rotates counterclockwise without sliding. Figure 13(a) shows the view parallel to the $\boldsymbol{e}_3$ axis. Initially, the $\bar{\boldsymbol{e}}$ and $\boldsymbol{e}$ systems are matched, then as shown in Fig. 13(b), if the straw rotates counterclockwise, the rod is fixed and the contact point moves and is now at P_1'. The contact point P_1 before the rotation is P_{1r} as a point on the face of the rod and P_{1c} as a point on C_1. Because the straw is rotating and does not slip, the curved distance between points $P_1'P_{1r}$ and $P_1'P_{1c}$ is the same. Because $\boldsymbol{e}_1$ is defined as an axis that always points toward the contact point, $\boldsymbol{e}_1$ in Fig. 13(b) rotates counterclockwise from $\boldsymbol{e}_1$ in Fig. 13(a). Let this angle be $\frac{\pi}{2}$, for example. However, $\bar{\boldsymbol{e}}_1$ also rotates counterclockwise, but the angle is less than $\frac{\pi}{2}$. The reason for the difference in the angle is that the radius of the rod is different from the radius of C_1. Figure 14 shows the motion of the rod and C_1 from an oblique top view.

Next, let us consider the case where the straw is in motion, tilted against the rod and in contact at three points. Because they are in contact at three points, they are tilted at a certain angle ψ, and this angle remains constant during the rotation. Consider the case where the straw rotates counterclockwise and the contact points $P_{(i=1,2,3)}$ change to $P'_{(i=1,2,3)}, P''_{(i=1,2,3)}$ as shown in Fig. 15(a)–(c). The lines between (a) and (b) and those between (b) and (c) in Fig. 15 show the same heights, indicating that the straw is rising as it rotates counterclockwise at $\psi < 0$.

Let us consider whether the straw is slipping by determining how far each contact point moves. Figure 16(a) and (b) show the views parallel to the $\boldsymbol{e}_3$ axis, so the cross section of the rod is an ellipse. The straw is fixed and drawn as if the rod is moving. In Fig. 16(a), P_i, P_i', P_i'' $(i = 1, 2)$ of Fig. 15 are projected onto the C_1 plane as $\bar{P}_i, \bar{P}_i', \bar{P}_i''$ $(i = 1, 2)$.

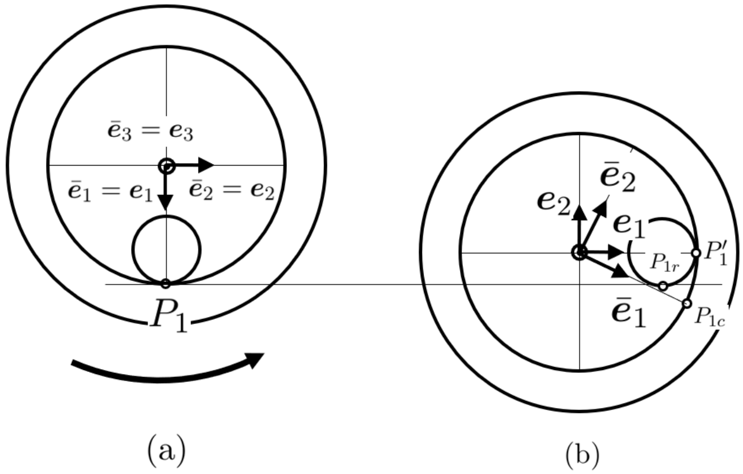

FIG. 13. (a) View parallel to $\boldsymbol{e}_3$ axis. Initially, the $\bar{\boldsymbol{e}}$ and $\boldsymbol{e}$ systems are matched, and the contact point is P_1. (b) The new contact point after rotation is P_1', and the contact point before rotation P_1 is P_{1r} as a point on the face of the rod and P_{1c} as a point on C_1.

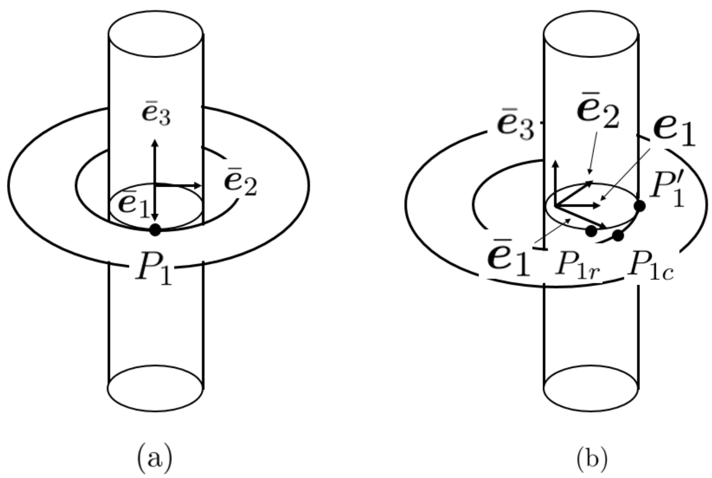

FIG. 14. (a) and (b) are oblique top views of Fig. 13(a) and (b), respectively.

In Fig. 16(b), if the angle between the line segment connecting the origin G and the point $\bar{P}_1$ and the line segment connecting the origin G and the point $\bar{P}_1''$ is γ, then so is the angle between the line segment connecting the origin G and the point $\bar{P}_2$ and the line segment connecting the origin G and the point $\bar{P}_2''$. This is because the triangles $G\bar{P}_2\bar{P}_1$ and $G\bar{P}_2''\bar{P}_1''$ are congruent. Then the length of the arc $\bar{P}_1\bar{P}_1''$ is $\bar{l}_1\gamma$ and the length of the arc $\bar{P}_2\bar{P}_2''$ is $\bar{l}_2\gamma$. The actual distance moved by the contact point must include the height moved in the $\boldsymbol{e}_3$ axial direction, and this is x for both arcs. The actual distance moved is $P_1P_1'' = \sqrt{(\bar{l}_1\gamma)^2 + x^2}$ and $P_2P_2'' = \sqrt{(\bar{l}_2\gamma)^2 + x^2}$, respectively, and $\bar{l}_1 \neq \bar{l}_2$, so the distance is different. Thus, if P_1 does not slip, then P_2 and P_3 do, and if P_2 and P_3 do not slip, then P_1 does. There may be other cases, but investigating which cases occur is left for future work because it is difficult to confirm with small objects such as straws.

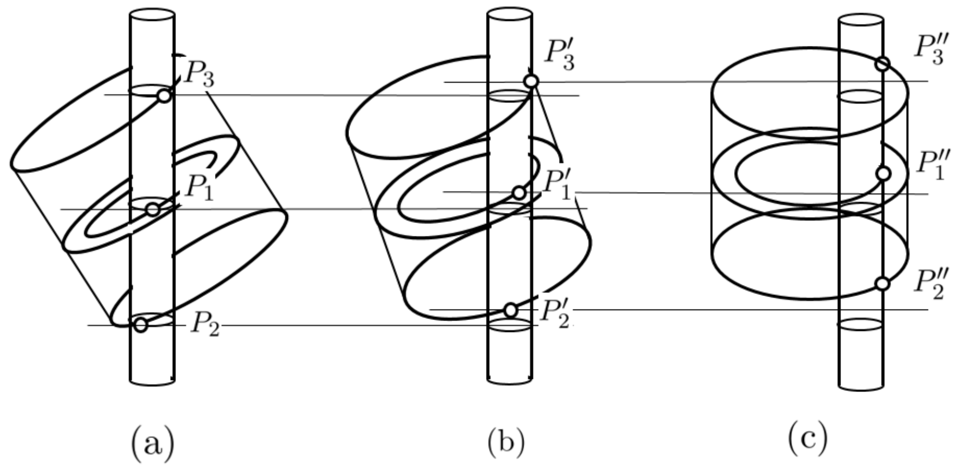

FIG. 15. (a)–(c) show the straw rotating counterclockwise and the contact point P_i changing to P'_i, P''_i. The lines between (a) and (b) and those between (b) and (c) show the same heights, indicating that the straw is rising as it rotates counterclockwise at $\psi < 0$.

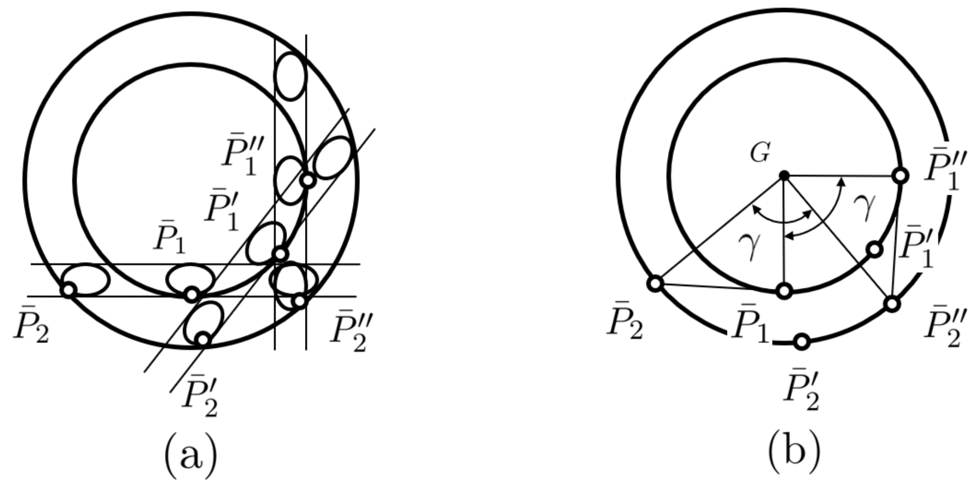

FIG. 16. Views parallel to $\boldsymbol{e}_3$ axis. The straw is fixed and drawn as if the rod is moving. (a) P_i, P'_i, P''_i $(i = 1, 2)$ of Fig. 15 are projected onto the C_1 plane as $\bar{P}_i, \bar{P}'_i, \bar{P}''_i$ $(i = 1, 2)$. (b) The angle between the line segment connecting the origin G and the point $\bar{P}_1$ and the line segment connecting the origin G and the point $\bar{P}''_1$ is γ.

We do not know at which contact point the straw is slipping; however, because it is in contact with the rod at three points, the straw rotates at a fixed angle ψ to the rod. It is important that the angle is fixed at ψ. The counterclockwise-rotating straw rises if $\psi < 0$ and falls if $\psi > 0$. When the descending straw (with $\psi > 0$) touches the reflector, the inclination of the straw to the rod changes (to $\psi < 0$) and it begins to rise again.

Meanwhile, similar motion occurs in the case of a rod through a washer. As analyzed previously by the present author [13], the washer exhibits two types of motion while rotating: staying in place like a hula hoop or moving unidirectionally. As shown elsewhere [14], the motion of small toy rings known as jitter or chatter rings corresponds to the unidirectional motion of the washer along the rod. In hula-hoop motion, there is one point of contact between the washer and the rod, but in unidirectional motion, there are two points of contact. Because they are in contact at two points, the angle between the rod and the washer is constant, and the washer moves unidirectionally as it rotates. A washer making two points of contact with a rod so that the angle is constant and the washer moves unidirectionally is very similar to a straw making three points of contact so that the angle is constant and the straw moves unidirectionally.

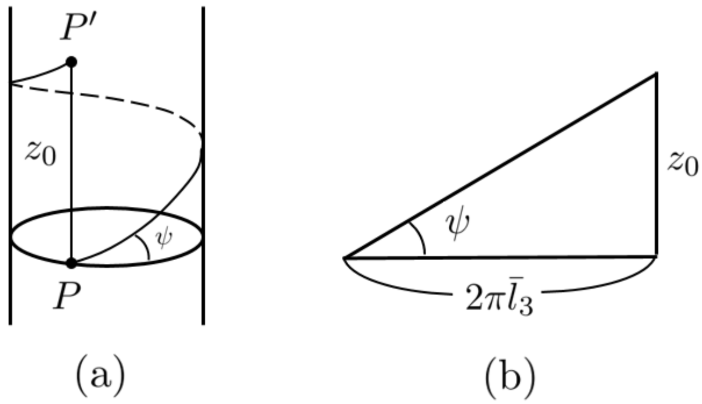

FIG. 17. (a) Straw rotates around rod, and contact point P on rod surface makes one rotation as it rises to P'. The distance risen after one rotation is that between P and P', which is $z_0 > 0$. (b) Net diagram of (a).

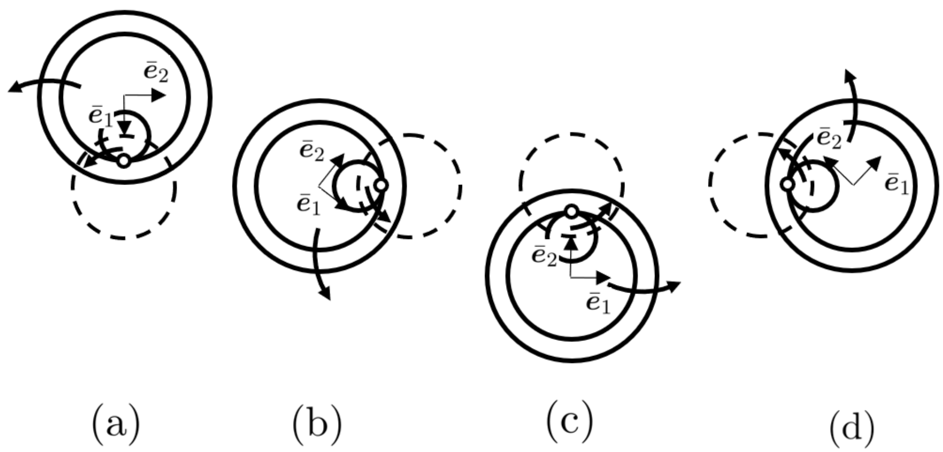

FIG. 18. Dotted line is orbital path of rod, which turns counterclockwise. The small white circle is the contact point, and $\bar{\boldsymbol{e}}_{1,2}$ are the principal axes of inertia of the straw. (a) and (b) correspond to Fig. 13(a) and (b), respectively, and (c) and (d) show the contact point rotated by π and $\frac{3}{2}\pi$, respectively.

B. Relationship Between Velocity and Length of Straw

As introduced in Section II B, the paper cup moved well when a rubber strip was placed inside it to prevent sliding, so in the following discussion we assume no sliding at contact point P_1 but sliding at P_2 and P_3.

The vertical velocity of the straw is related to the angle ψ between it and the rod. Figure 17(a) shows the situation in which the straw rotates around the rod and the contact point P on the surface of the rod makes one rotation as it rises to P'. The distance risen after one rotation is that between P and P' in Fig. 17(a), which is $z_0 > 0$. Figure 17(b) is a net diagram of Fig. 17(a), and because the radius of the rod is $\bar{l}_3$, z_0 is given by

$$z_0 = -2\pi\bar{l}_3 \tan\psi > 0. \tag{5}$$

If the number of times that the contact point rotates around the rod per second can be found, then the velocity can be determined. This number of rotations equals that of the nut (n), which is explained as follows. Video evidence shows that the orbital rotation of the rod is synchronized with the rotation of the straw and the contact point. Figure 18 is a conceptual diagram of the synchronization of the orbital rotation of the rod with the rotation of the straw and the contact point. The straw is tilted by angle ψ relative to the rod, but for simplicity the effect of the tilt is omitted in this conceptual diagram. The dotted line is the orbital path of the rod, which turns counterclockwise. The small white circle is the contact point, and $\bar{\boldsymbol{e}}_{1,2}$ are the principal axes of inertia of the straw. Figure 18(a) and (b) correspond to Fig. 13(a) and (b), respectively, and Fig. 18(c) and (d) show the contact point rotated by π and

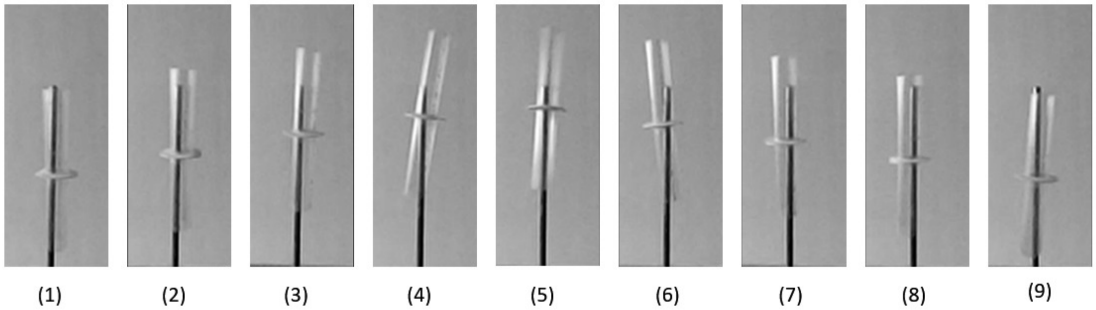

FIG. 19. Motion of straw near rod tip.

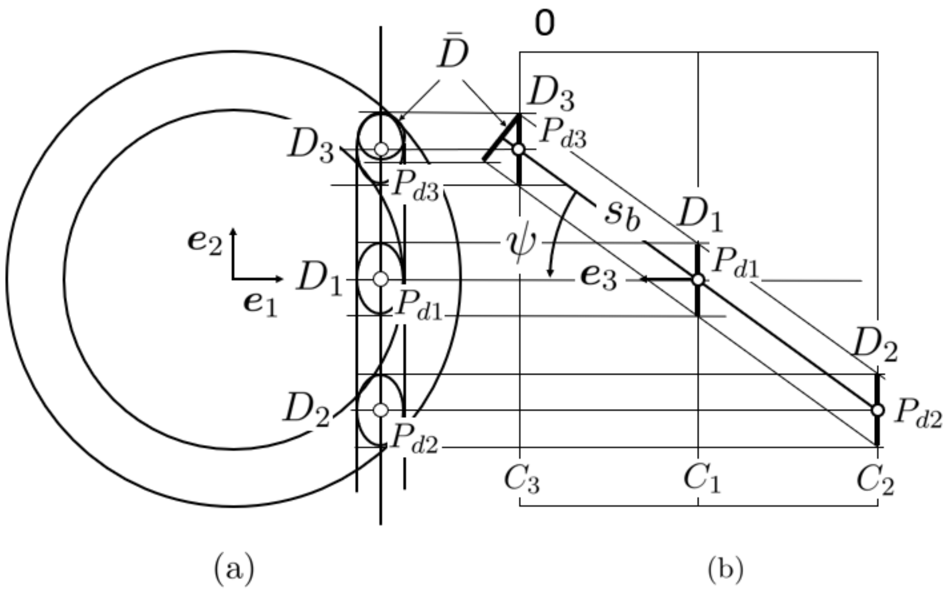

FIG. 20. View of rod inside straw. (a) D_1, D_2, D_3 are the cross sections of the rod formed by the $\boldsymbol{e}_1, \boldsymbol{e}_2$ planes at the contacts P_1, P_2, P_3 and are ellipses. Let P_{d1}, P_{d2}, P_{d3} be the center points of these ellipses D_1, D_2, D_3. Also, the cross section at the rod tip is $\bar{D}$. (b) The circumferences C_1, C_2, C_3 [Fig. 9(b)] are indicated by vertical lines. The line through P_{di} $(i = 1, 2, 3)$ is the line through the center of the rod, which is s_b. The angle between this line and the line parallel to the $\boldsymbol{e}_3$ direction is ψ.

$\frac{3}{2}\pi$, respectively. Figure 18(a)–(d) show that as the rod orbits once, the contact point makes one rotation. On the other hand, because the orbital rotation of the rod and the rotation of the nut are also synchronized, the number of orbits of the rod is equal to the number of rotations of the nut (n), and so the number of rotations of the contact point equals n. Finally, the rise velocity v_s of the straw is obtained using n and Eq. (3) as follows:

$$v_s = nz_0 = -2\pi n\bar{l}_3 \tan\psi = 2\pi n\frac{\bar{l}_3}{\bar{l}_4}\sqrt{(\bar{l}_2 - \bar{l}_3)^2 - (\bar{l}_1 - \bar{l}_3)^2}. \tag{6}$$

C. Analysis of Reversal of Motion at Rod Tip

Next, let us consider why the straw reverses its motion at the rod tip. As shown in Fig. 19, the straw does not descend as soon as it reaches the rod tip; rather, the rod tip enters the straw, and the latter begins to descend at a certain point thereafter.

Figure 20 shows the situation in which the straw is rising and the rod tip is at the top end of the straw; Fig. 20(a) is a top view and Fig. 20(b) is a view from right beside the straw. We will show the relationship between ψ and the position of the rod tip. Because ψ is the angle between the line through the center of the rod and the line parallel to the $\boldsymbol{e}_3$ direction, the former must be illustrated. In Fig. 20(a), D_i $(i = 1, 2, 3)$ are the cross sections of the rod formed

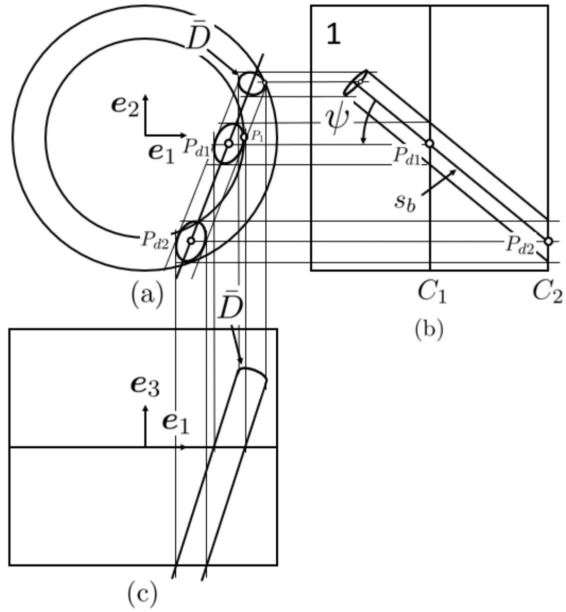

FIG. 21. View of rod inside straw (1). The symbols are the same as those in Fig. 20.

by the $\boldsymbol{e}_1, \boldsymbol{e}_2$ planes at the contact points P_i $(i = 1, 2, 3)$, respectively, and are ellipses. Denote as P_{di} $(i = 1, 2, 3)$ the center points of these ellipses D_i $(i = 1, 2, 3)$, respectively. Also, the cross section at the rod tip is $\bar{D}$. In Fig. 20(b), the circumferences C_1, C_2, C_3 [Fig. 9(b)] are indicated by vertical lines. The line through P_{di} $(i = 1, 2, 3)$ is the line through the center of the rod, which is s_b. The angle between this line and the line parallel to the $\boldsymbol{e}_3$ direction is ψ. Then, as it continues to rise, contact point P_3 moves into the interior of the straw, and Fig. 21(a)–(c) illustrate this situation. The intersection of the horizontal line extending from the center point of the rod P_{d1}, P_{d2} in Fig. 20(a) and the circumference of the straw C_1, C_2 (vertical line) is the location of the center point P_{d1}, P_{d2} in Fig. 20(b). Therefore, the straight line through P_{d1}, P_{d2} in Fig. 20(b) is s_b, and the angle between this line and the line parallel to the $\boldsymbol{e}_3$ direction is ψ. The gradual lowering of the rod tip is illustrated in Figs. 21–27.

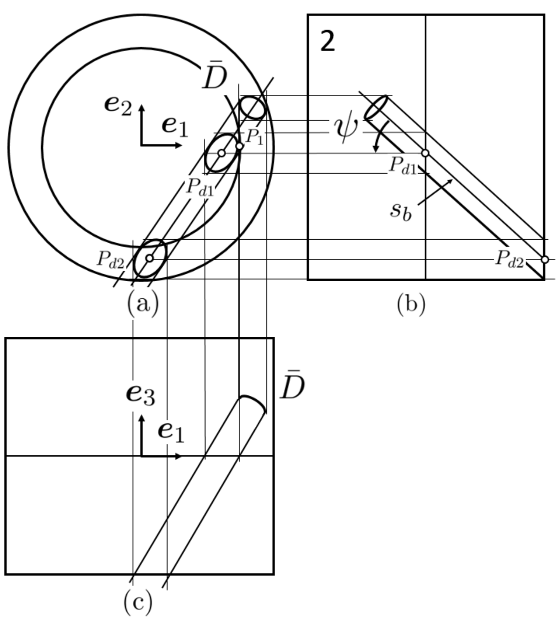

FIG. 22. View of rod inside straw (2).

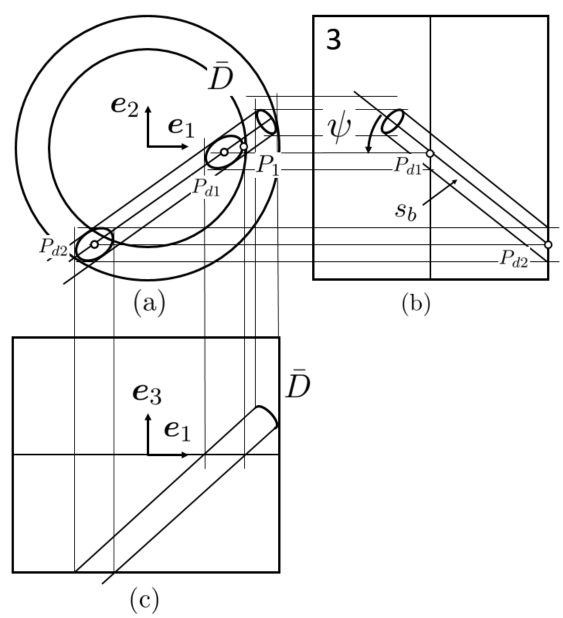

FIG. 23. View of rod inside straw (3).

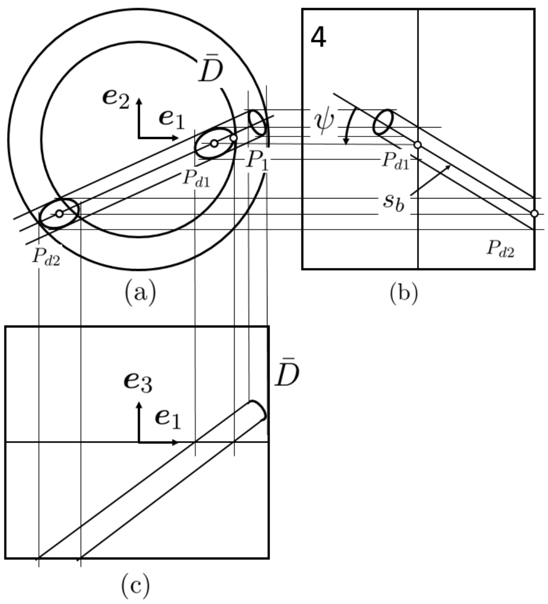

FIG. 24. View of rod inside straw (4).

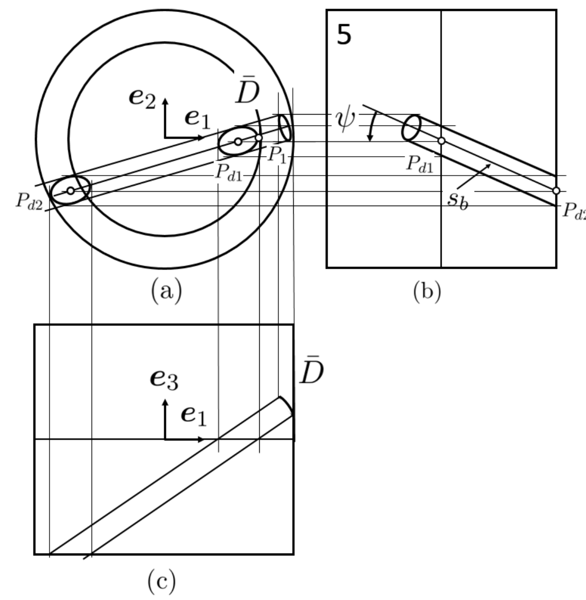

FIG. 25. View of rod inside straw (5).

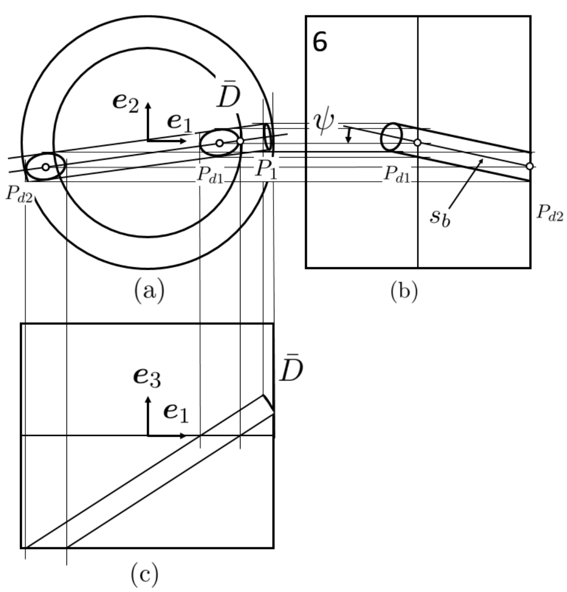

FIG. 26. View of rod inside straw (6).

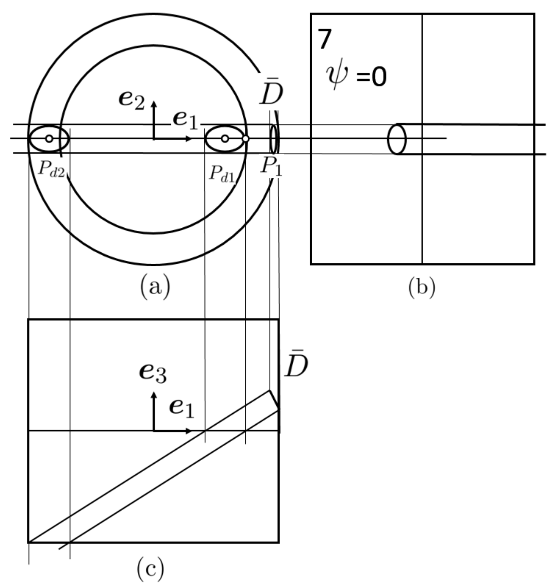

FIG. 27. View of rod inside straw (7).

Regarding the line s_b passing through the center of the rod, Figs. 20(b)–27(b) are collected in Fig. 28, which shows the ψ transition. The numbers in Fig. 28 correspond to the numbers in the captions of Figs. 20(b)–27(b). Starting from ψ in Fig. 20 (corresponding to 0), the angle increases slightly in Fig. 21 (corresponding to 1) and Fig. 22 (corresponding to 2). It then begins to decrease, and the velocity decreases accordingly. The angle is $\psi = 0$ in Fig. 27 (corresponding to 7). The straw stops rising here and then turns downward because $\psi > 0$.

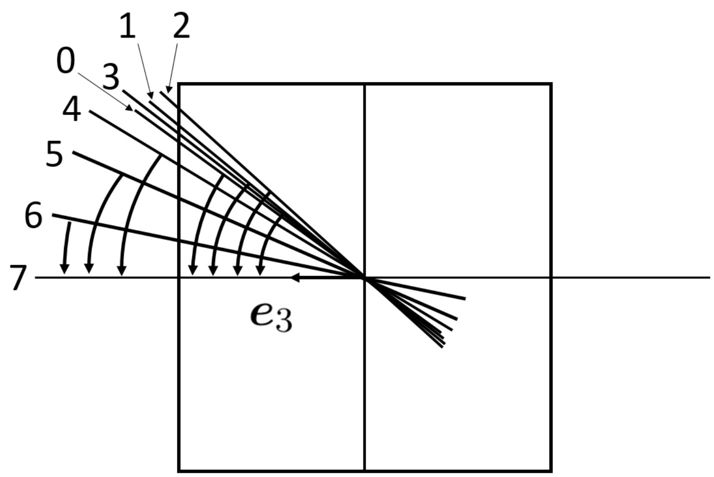

FIG. 28. This figure was drawn by collecting the line s_b passing through the center of the rod, from which the change in angle ψ can be read. The numbers correspond to those in the captions of Figs. 20(b)–27(b).

Finally, as the straw rises, the rod tip enters the straw. As it does, the angle ψ between the rod and the straw approaches zero and the velocity decreases. When ψ reaches zero, the rise stops, the sign of ψ is reversed, and the straw begins to descend. This is the mechanism by which the straw returns from the tip of the rod.

IV. COMPARISON OF THEORETICAL AND EXPERIMENTAL VELOCITIES

From Eq. (6), the vertical velocity of the straw is a function of the straw half-length $\bar{l}_4$ and the nut rotation number n when the straw radii $\bar{l}_1$ and $\bar{l}_2$ and the rod radius $\bar{l}_3$ are fixed. Therefore, the theoretical velocity can be obtained by measuring $\bar{l}_i$ ($i = 1 \sim 4$), finding n from video footage, and substituting into Eq. (6). Let us compare this theoretical velocity with that obtained experimentally from video footage. Thus far, we have focused on the straw moving vertically, but because gravity might affect the vertical velocity, we oriented the rod horizontally and measured the straw's velocity as it moved in the left–right direction.

The straw shown in Fig. 6(b) consisted of two short straw segments joined by a paper disk that contained a small circular hole. However, the hole was not exactly circular because it was made using a utility knife, and there was no guarantee that (i) the central axes of the hole and the straw were aligned accurately and (ii) the straw and the paper disk were perpendicular to each other. Normally, one aims to conduct experiments with accurately prepared materials, but as is usually the case, one experiments initially with the materials at hand. A search was then made for another type of straw, and one was found that already had a slightly rounded tip with a smaller diameter, as shown in Fig. 29. Two sections of this type of straw were prepared, and their rounded portions were aligned and glued together by clipping them together with a brace to form a straight line. The measured values of $\bar{l}_1$, $\bar{l}_2$, and the radius $\bar{l}_3$ of the rod in this straw were $\bar{l}_1 = 2.5$ mm, $\bar{l}_2 = 3.0$ mm, and $\bar{l}_3 = 1.0$ mm.

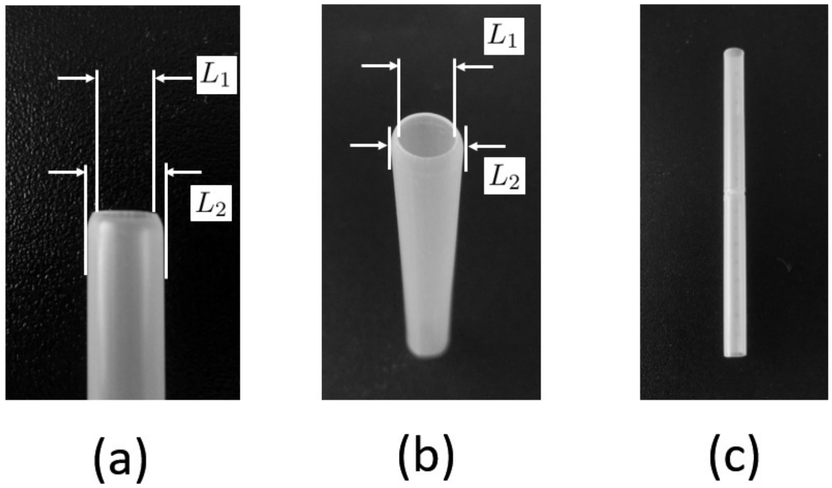

FIG. 29. Straw with a slightly rounded and narrower tip: (a) side view (outer diameter $L_2 = 2\bar{l}_2 = 6.0$ mm; inner diameter $L_1 = 2\bar{l}_1 = 5.0$ mm); (b) oblique view from above; (c) two sections of this straw joined together.

The straw half-length $\bar{l}_4$ was reduced from 4.5 cm to 1 cm in intervals of approx. 0.5 cm and then to approx. 0.8, 0.6, and 0.4 cm. Straws with $\bar{l}_4 > 5$ cm did not produce good side-to-side motion, which is why it was decided to use straws with $\bar{l}_4 \leq 4.5$ cm. The exact value of $\bar{l}_4$ was measured with calipers because changed upon cutting the straw sections with scissors. Because the two straw sections differed slightly in length, $\bar{l}_4$ was taken as the average value.

When the rod attached to the motor vibrated, nodes and antinodes were created along the rod, as shown schematically in Fig. 30. The nodes affected the straw by slowing it down and sometimes even causing it to stop. A more accurate experiment would have involved equipment with a mechanism to rotate the rod without nodes forming, but first the experiment was conducted using the motor and rod from the demonstration. The rod with a length of approx. 38 cm allowed a straw with $\bar{l}_4 = 4.5$ cm to be measured. To reduce the influence of node c in Fig. 30, the velocity at which the left end of the straw passed a region 2–3 cm from point a was measured. The velocities of the straw moving to the left and right were measured three times each, then the straw was removed from the rod and replaced in the opposite orientation, whereupon the measurements were repeated, resulting in 12 in total. The final velocity was the average of those 12 measurements, with the error calculated from the deviations from the average.

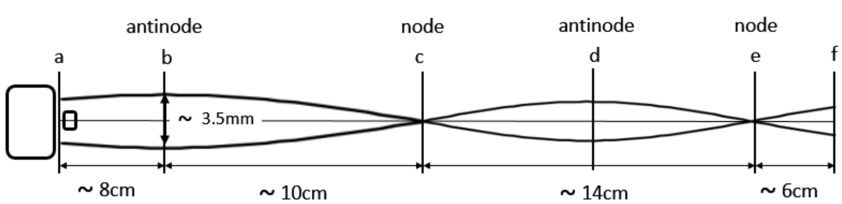

FIG. 30. Schematic of nodes and antinodes on vibrating rod. The distances for ab, bc, ce, and ef are approx. 8, 10, 14, and 6 cm, respectively, and the antinode amplitude is approx. 3.5 mm.

A ruler was placed parallel to the rod as shown in Fig. 31, and the straw motion was captured at 1,000 fps with a digital camera (CASIO EX-ZR200). This video was then analyzed using video editing software (DaVinci Resolve). The frame numbers were read when the left edge of the straw reached reference line A [Fig. 32(a)] and line B at a distance of 1 cm from line A [Fig. 32(b)], then the experimental velocity was obtained from the known position and time differences. Furthermore, the number of nut rotations n was also obtained from the video, and using this and the measured value of $\bar{l}_4$, the theoretical velocity was obtained using Eq. (6).

For the three straws produced in the same way and used in the experiment, Figs. 33–35 show the theoretical velocity v_{th} and the experimental velocity v_{exp} plotted against $\bar{l}_4$, with error bars for v_{exp}. In all three cases, the theoretical values are larger than the measured values, presumably because although in theory a straw does not slide at the point of contact between its center and the rod, in reality it does slide. In Section II B, the motion of two paper cups

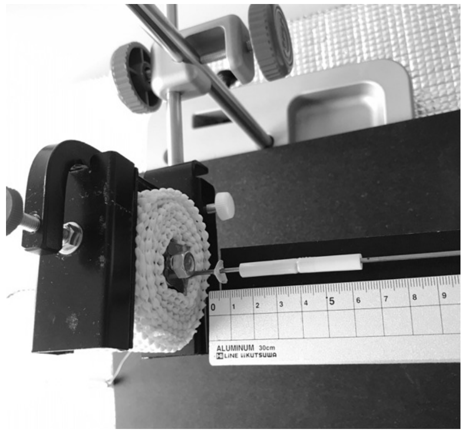

FIG. 31. A ruler was placed parallel to the rod, and video was taken with a digital camera from above.

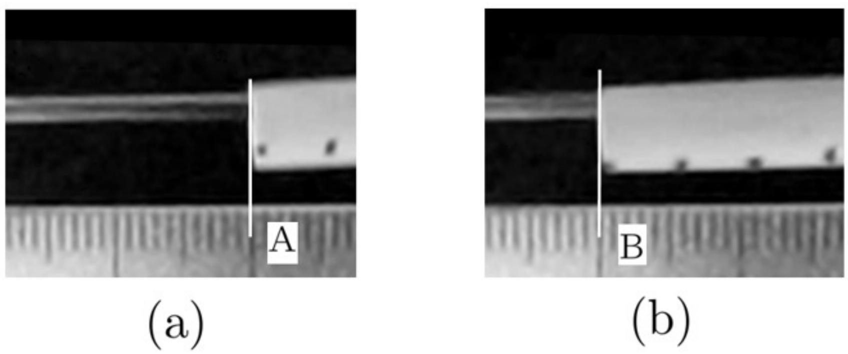

FIG. 32. Still images of straw reaching reference lines A and B on ruler parallel to rod: (a) frame with straw moving to the left and reaching line A; (b) frame with straw moving to the left and reaching line B.

agitated by hand was discussed: the paper cup with no rubber strip inside it slipped on the rod, and the same thing is assumed to be happening in the case of the straws. However, the theoretical and experimental velocities decrease in similar ways with increasing $\bar{l}_4$, and their agreement is determined by the relative error $\delta = 1 - v_{exp}/v_{th}$. For each straw, a graph of δ versus $\bar{l}_4$ is shown in Fig. 36.

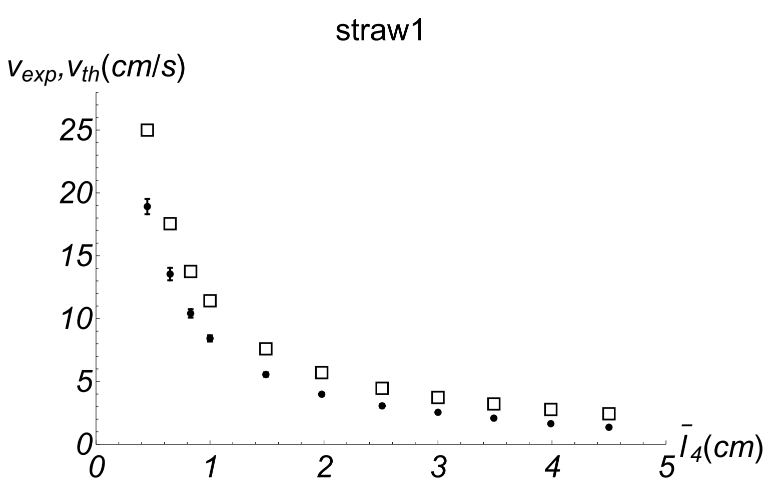

FIG. 33. Theoretical (□) and experimental (•) results for straw 1. For the experimental results, the error bars become smaller than the data points at larger values of $\bar{l}_4$.

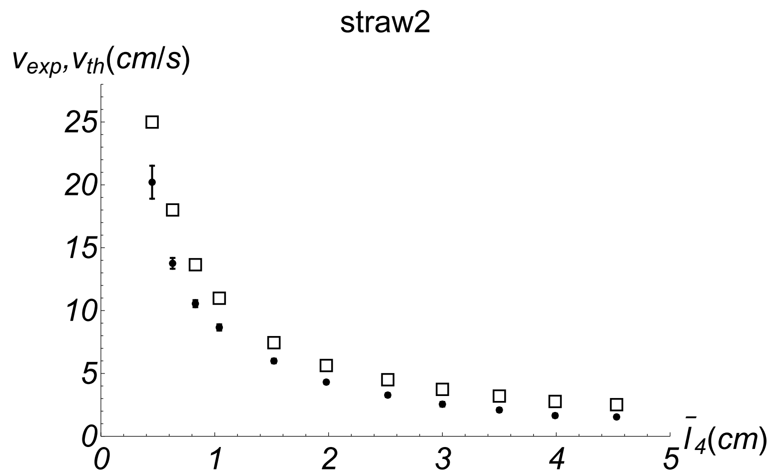

FIG. 34. As Fig. 33 but for straw 2.

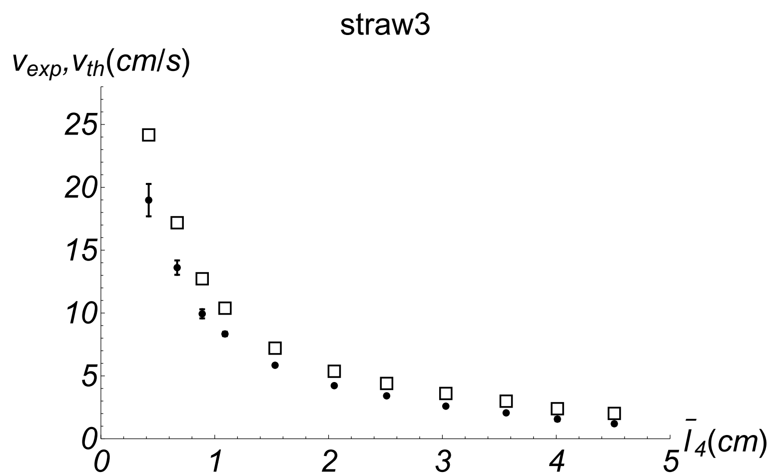

FIG. 35. As Fig. 33 but for straw 3.

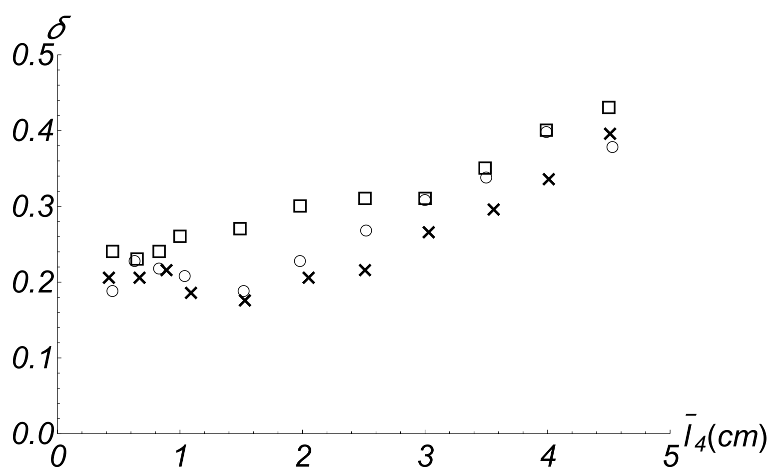

FIG. 36. Relationship between $\bar{l}_4$ and relative experimental error δ for straw 1 ($\square$), straw 2 ($\circ$), and straw 3 ($\times$).

To see why v_{exp} is smaller than v_{th} when sliding occurs, consider the trajectory of the contact point P on the rod. Without sliding friction, P' goes around and back to P in Fig. 17, and we have $z_0 = 0$. With sliding friction, the trajectory of P is considered to be a straight line or curve with slope less than $\tan\psi$ at the point where it slides, e.g., Fig. 37. Then, because the distance z_0' is smaller than z_0 and $z_0' = \rho z_0$ ($\rho < 1$), the experimental velocity v_{exp} is

$$v_{exp} = nz_0' = \rho n z_0 = \rho v_{th} \tag{7}$$

and the relative error is $\delta = 1 - \rho$. If ρ is not a function of $\bar{l}_4$ but is constant, then so is δ.

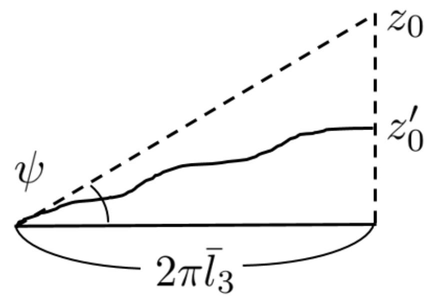

FIG. 37. Trajectory of contact point P on rod if it slips in places.

The experimental values show that the relative error for all three straws decreases as $\bar{l}_4$ decreases from 4.5 cm to 1.5 cm, and the agreement with the theoretical values improves. However, below 1.0 cm, the values oscillate around 0.24, 0.21, and 0.21 (mean relative error) for straws 1, 2, and 3, respectively, showing approx. 80% agreement. The averages for all lengths are 0.30, 0.27, and 0.25 for straws 1, 2, and 3, respectively, and these average to 0.27, indicating approx. 73% agreement.

There are two possible reasons for the larger relative error and worse agreement with theoretical values as the half-length increases above 1.5 cm: (i) nodal effects from the rod and (ii) bending deformation of the straw. As the half-length increases, the right end of the straw is closer to node c in Fig. 30 and is considered to be affected by it. In addition, the two straw halves are joined at the center with glue, but this glue may stretch and bend if force from the rod is applied to the two ends. Figure 38(a) shows that the straw bends in the center and splits into two pieces, creating a new inner circumference C_1' that is in contact with the rod at P_1'. The angle between the axis perpendicular to the circumference C_1 and the centerline of the rod is ψ.

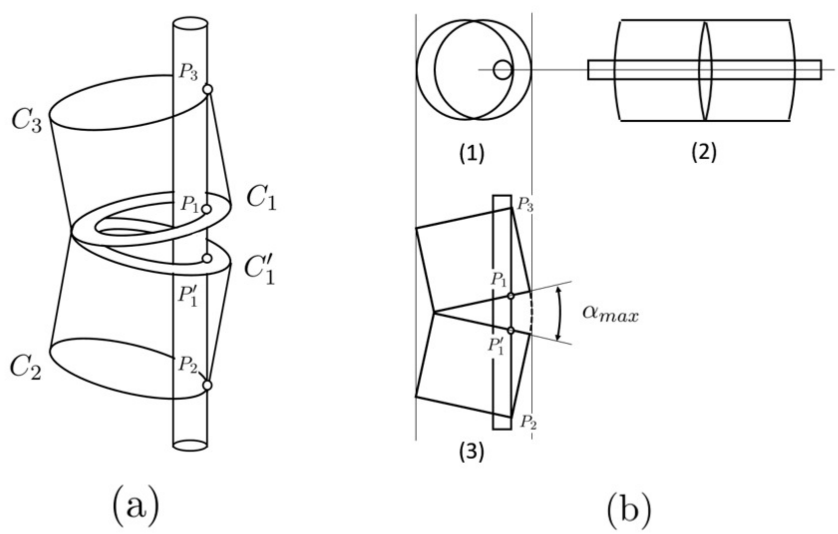

FIG. 38. (a) Straw bends in center and splits into two pieces, creating a new inner circumference C_1' that is in contact with the rod at P_1'. (b) The maximum bend angle is α_{max}, with $\psi = 0$.

Figure 38(b) shows the situation for maximum bend angle α_{max} and $\psi = 0$. If the straw bends at an angle α, then the angle ψ corresponding to α is less than ψ_{th}. This is because we have $\psi = 0$ when the bend angle is maximum, and

ψ_{th} obtained by Eq. (4) is maximum when the bend angle is zero. Therefore, if the straw bends, then it will move slower than the theoretical velocity. As can be seen from Fig. 38(b3), a longer straw requires a smaller bend angle to reach $\psi = 0$, so for a given bend angle α, ψ is smaller for a longer straw. Therefore, the longer the straw, the slower it is expected to move.

As already mentioned, to obtain good agreement between theoretical and experimental values would require an experimental setup in which the nodes and antinodes were absent. Additionally, the item that moves along the rod should not be created by joining two straws together; rather, it should be made of a material that does not slip on the rod and is not deformed as one piece. Experimenting with such equipment and items is a future challenge. Nevertheless, although challenges remain, the agreement between the theoretical values and the present experimental values is approx. 73%, and this agreement would be even better if not for the effects of sliding, the presence of nodes and antinodes, and bending deformations. Therefore, the experimental values seem to support the validity of the straw motion considerations and the theoretically derived Eq. (6).

V. CONCLUSION AND DISCUSSION

When a straw with an articulated section is slid over a vertical rod vibrated by a motor, the straw moves up and down. The present author speculated that this movement is caused by the center of the straw being narrower than the ends, so a straw with such a shape was created and attempts were made to move it. Having found the same motion, the mechanism for vertical motion of a straw whose center is narrower than the ends was examined. Assuming that the rod and the straw are in contact at three points (i.e., at both ends and the center) and that the straw does not slide at the center contact point but does slide at the ends, the angle ψ between the rod and the straw becomes constant. Therefore, when the straw rotates against the rod, it will move unidirectionally. Also, as the straw rises, the rod tip enters the straw. Because contact is still made at three points in this situation, the angle ψ between the rod and the straw decreases and becomes zero. Because the rate of ascent is proportional to ψ, the ascent stops when ψ reaches zero, and then the sign of ψ reverses, which means that the straw begins to descend and returns to the bottom of the rod. When the straw contacts the reflector at the bottom, the sign of ψ reverses again and the straw begins to rise and repeats the same movement. This is the mechanism for the up-and-down movement of the straw.

Experiments were conducted to measure the velocities of three straws of different lengths, and the results showed that the theoretical velocities were greater than the experimental ones. The reason for this was assumed to be that although in theory the straw does not slip at the point of contact between its center and the rod, in reality it does slip. However, the theoretical and experimental velocities decreased in similar ways with increasing $\bar{l}_4$, and the agreement between them was determined by the relative error. For half-lengths less than 1.0 cm, the agreement averaged approx. 80%, and for all lengths the agreement averaged approx. 73%. The agreement would have been even better had it not been for the effects of slipping between the straw and the rod, the presence of the nodes and antinodes of the rod's vibration, and deformation in the central part of the straw. Considering these effects, the experimental values support the validity of the mechanistic considerations of the straw motion and the theoretically determined velocities.

To eliminate the effects from the nodes and antinodes caused by the vibration of the rod, it is necessary to construct an experimental setup that does not allow for the formation of nodes and antinodes. In addition, the item that moves on the rod should not be made by joining two straw sections together; rather, it should be made of a material that does not slip on the rod and does not deform as a single unit. Future work will be to obtain experimental values with such experimental equipment and items and to compare them with theoretical values.

ACKNOWLEDGMENTS

The author thanks H. Nakano (Niigata University) for informing him that K. Sato's work is at the Niigata Science Museum and K. I. Aoki (Kanazawa University) for informing him that it is at the Bando Kobe Science Museum. The author also thanks the staff of the Museum of Fine Arts, Gifu, who told us about the internal structure of the Styrofoam of the gifu-susuki-clump'99. Finally, the author thanks K. Ishikawa (heir to the copyright of Keijiro Sato's works) for sending him materials related to K. Sato.

CONFLICT OF INTEREST

The author declares no conflicts of interest associated with this manuscript.

[1] Keijiro Sato He is a composer and kinetic artist. (1927–2009). His works are in the collection of the Museum of Fine Arts, Gifu.
[2] "Gifu Susuki Clump'99 (Susuki: Pampas Grass)" https://www.ntticc.or.jp/en/archive/works/gifu-susuki-clump-99-susuki-pampas-grass/ https://satoh-keijiro.jpn.org/gifu-susuki99/
[3] "Motion of a styrofoam sphere through a vibrating rod" https://youtu.be/P52kCnPnn5w
[4] H.Takano: "Motion of straws with different radii at both ends through a vibrating rod" in preparation.
[5] Vertical motion(the tip of the rod is up) https://youtu.be/kZ4-EjJ-G9I
[6] "Horizontal motion" https://youtube.com/shorts/T2MREf3Re6M?feature=share
[7] "Vertical motion(the tip of the rod is down)" https://youtube.com/shorts/LdhBp0E-hNI?feature=share
[8] "Motion of a straw with a small radius at the center" https://youtu.be/FN1HaecUY7I
[9] "Motion of straws with different radii at both ends 1" https://youtu.be/V3JZPwuFig8
[10] "Motion of straws with different radii at both ends 2" https://youtu.be/Uh5BtW14dXg
[11] "Motion of one paper cup" https://youtu.be/RjnxDmwZedY
[12] "Motion of two paper cups" https://youtu.be/StdNC-oOB7E
[13] Analyzing the Motion of a Washer on a Rod(2023), Regular and Chaotic Dynamics Vol.28(No.2) 227-250 https://www.juen.ac.jp/lab/takano/chatterring/WasheronRod.pdf
[14] JCRA: Japan Chatter Ring Association. http://jaringa.web.fc2.com/index-e.html